# Electrical discharge consolidation of Al and Ti powders

F. Ternero[1*], R.M. Aranda[2], P. Urban[1], R. Astacio[1] and J.M. Montes[1]

*[1]Advanced Materials Engineering Group, Escuela Técnica Superior de Ingeniería,*
*Universidad de Sevilla, 41092 Sevilla, Spain*
*[2]Advanced Materials Engineering Group, Escuela Técnica Superior de Ingeniería,*
*Universidad de Huelva, 21071 Huelva, Spain*

## Abstract

In this paper, electrical-discharge-consolidation (EDC technique) experiments were carried out with an equipment based on the technology developed for the stud welding technology. The main advantage of the EDC technique is its high speed, on the order of milliseconds or less, which makes it particularly interesting when a high final porosity is aimed, or when the inherent nanostructure of the powders needs to be preserved. Compacts of Ti and Al were consolidated with this technique, both directly from loose powders and from cold pressed green compacts. Two different configurations (200 V – 66 mF and 800 V - 1.1 mF) were tested. Relative density, microhardness, electrical resistivity and metallographic and SEM studies were carried out to understand the changes in powder particles caused by the electrical discharge. The use of a high capacity in the capacitors bank, despite the use of a lower voltage, results in a better consolidation process.

*Keywords: Electrical Discharge Consolidation; Capacitors bank; Porosity; Al powder; Ti powder.*

## 1. Introduction

The conventional powder metallurgical processing route essentially consists of cold compaction of a mass of metal powder to obtain a green compact, followed by furnace sintering to provide the final or near-final part. Although this is the route most frequently used in the industry, new alternatives are constantly being investigated to improve, at least partially, the problems and shortcomings of the current technology. In this sense, the direct use of electricity as a means of consolidating powders (metallic and ceramic) has been suggested on numerous occasions.

The great diversity of proposed methods can be grouped under the generic name of Electric Current Assisted Sintering Techniques (ECAST) or by the term FAST (Electric Field Assisted Sintering Techniques). In fact, the speed of the processes is the most remarkable feature and the common factor of all these techniques. In addition to the time savings, the high speed of electrical consolidation techniques represents an important advantage, as it often makes the use of vacuum or inert atmospheres unnecessary.

These techniques, like the conventional route, provide a part whose shape is virtually the final form. However, one of the problems frequently mentioned by researchers who have experimented with FAST techniques relates to the durability of the dies used, especially in cases where the die must be electrically insulating. The problem of choosing a material with acceptable durability and cost-effectiveness is of great interest and requires thorough study. Only with the satisfactory resolution of this problem will electrical consolidation techniques be able to find suitable niches for the industrial scale. However, on the laboratory scale, it is easy to find sufficiently acceptable solutions to work with.

In the so-called Electrical Discharge Consolidation (EDC), the electric current passing through the powder is also of high current intensity [11-18], however, compared to the ERS technique, the voltage can reach much higher values. This combination of high intensity and moderate (or high) voltage can be achieved by discharging the energy stored in a capacitor bank, a technique also known in the electrical field of welding. Because the electric current produces very fast micro-welds at the interparticle contacts, the required consolidation time can be extraordinarily short, as little as a few milliseconds or even microseconds. As Okazaki [11] concluded, the high speed of the EDC processes allows the nanostructure or amorphous character of the powders to be preserved, which is one of the most important advantages of the technique.

---

[*] Corresponding author. Tel.: +34954487305
E-mail fternero@us.es

In general, in the conventional route, the cold compaction step is sufficient to fracture and to partially remove the oxide (and/or hydroxide) layers surrounding the metal powder particles, although in cases where this process is not efficient, it may be useful to apply an extrusion process to the powders. The removal of oxide layers in the EDC process is probably one of its greatest strengths and a consequence of the application of relatively high stresses. These voltages induce the dielectric breakdown of the layers, making them conductive and allowing the passage of a high current intensity [11]. The heat generated by this high electric current softens (or even melts) the metal under the oxide layer, so that it eventually fractures. Subsequent particle rearrangement processes remove the remaining oxides from the contact zones, a phenomenon that is effective even when no pressure is applied. Therefore, the EDC technique makes it possible to obtain compacts with high porosity. This presents an important difference between the EDC processes with respect to the ERS technique, where the initial resistivity of the powders is very high and hinders sintering, as the current intensity through the powder aggregate is negligible due to the lower voltage applied to the powder column, and not sufficient to break the oxide layers.

The main advantage of the EDC technique is an extraordinary short consolidation time (around milliseconds or microseconds), which makes unnecessary the use of vacuum or protective atmospheres. This fast process allows to preserve the inherent structure of the material and to obtain high-porosity compacts. This work describes the EDC experiments carried out with different powders (Al and Ti), and the obtained compacts properties are discussed.

## 2. Experimental Procedure and equipments

### 2.1. Description of the EDC Equipment

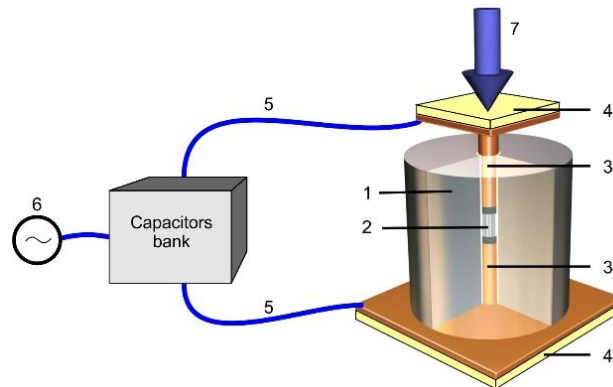Figure 1 shows a diagram of the basic components of the experimental equipment.



Figure 1. Diagram of the basic components of the EDC equipment: (1) thermally and electrically insulator die, (2) powder, (3) electrodes (upper and lower), (4) electric insulator (upper and lower), (5) connection wires to the capacitors bank, (6) external power supply (electrical network, 220 V), (7) pneumatic press.

Two different configurations were used: configuration I uses a charging voltage of 200 V and a capacitors bank with a capacitance of 66 mF, whereas configuration II uses a charging voltage of 800 V and a capacitance of only 1.1 mF. Both capacitors' banks were adapted from stud welding equipments.

### 2.2. Materials and Experimental Procedure

Two different commercial powders were studied: Al AS61 (with 0.15% Fe as main impurity) and Ti Sejong-325 (0.0038% Fe, 0.08% N, 0.035% Si, 0.003% Mn and 0.45% O).

These powders were analysed regarding their particle size by laser diffraction (Malvern Mastersizer 2000), and their morphology was studied by scanning electron microscopy (SEM, Philips XL-30 coupled with BSE and EDS detectors). Their compressibility curves were obtained by a compression test performed with a universal testing machine (Instron 5505). The powders absolute density was determined using a helium pycnometer (Accupy II1340).

Figure 2 shows the particle size distribution and compressibility curves of the two powders. Size distribution curves show a narrow and symmetric shape for the Al AS61 and Ti Sejong-325 powders. These morphological characteristics

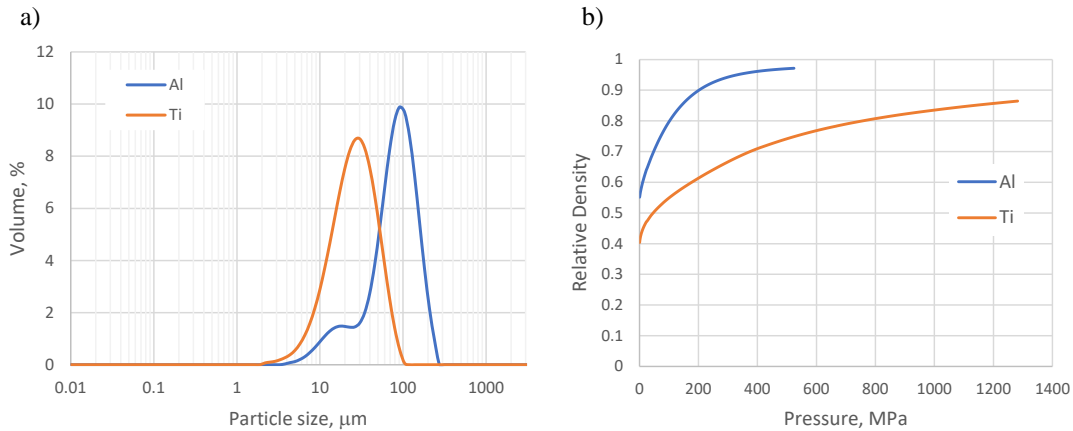were corroborated by SEM observation of the powders, as shown in Figure 3.

a)
b)



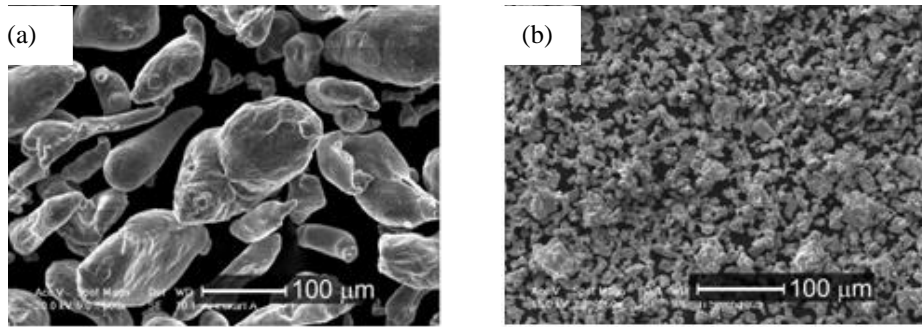Figure 2. (a) Granulometric, and (b) compressibility curves for Al and Ti powders.



Figure 3. SEM micrographs of studied powders: (a) Al AS61, (b) Ti Sejong-325.

EDC experiments were carried out both starting with loose powders and starting with cold pressed green compacts. In this last case, a cylinder die of 8 mm diameter was used to press the compacts. Compressibility curves show that different pressures are needed in the different powders in order to reach a similar initial *normalised porosity* (defined as the ratio between the porosity and the tap porosity) in green compacts. Initial relative porosities of 0.1 and 0.25 were chosen for Al powder, and 0.25 and 0.40 for Ti powder. Thus, two different pressures were applied to each powder: 990 and 490 MPa to Al and 1076 and 553 MPa to Ti powder. The pressure used for each type of powder depends on the properties of each powder to allow the compact to have sufficient consistency to be handled.

The powders (loose or pre-compacted) were subjected to electric discharge following three different vias: (1) discharging from configuration I (200 V-66 mF), (2) discharging with configuration II (800 V-1.1 mF) and (3) discharging with configuration II + I (one stage after the other).

The obtained compacts were characterised regarding their relative density (by weight and geometric measures), the Vickers microhardness HV (by Struers Duramin-A300) and the electrical resistivity (by the four probes method, Microhmmeter CA 10 Chauvin Arnoux). Moreover, diametrical sections of the compacts were observed by optical microscopy and fracture surfaces of mechanically broken compacts were studied by SEM.

## 3. Results and Discussion

### 3.1. Relative Density, Electrical Resistivity and Vickers Microhardness

Figure 4a, 4b and 4c respectively show relative density, microhardness and electrical resistivity of loose powders and higher-pressure pre-compacted compacts consolidated with configuration I (200 V-66 mF). For the pre-

compacted compacts, results are also shown in Figure 4d, 4e and 4f, both before the EDC (green compacts) and after the different discharge configurations.

As expected, EDC compacts obtained from loose powders show a lower relative density than the previously pressed ones (Figure 4a); this is due to the compaction pressure. The low density of the compacts prepared from loose powders is also accompanied by a low microhardness, as shown in Figure 4b, with a reduction of 20-40%. This is due to the higher porosity of these compacts, which also increases their resistivity, as shown in Figure 4c.

On the other hand, relative density and microhardness of pre-pressed compacts consolidated with configuration II (800 V-1.1 mF) result similar to these properties obtained in green compacts (Figure 4d and 4e). Both properties are improved when configuration I (200 V-66 mF) is used. Finally, compacts that were subjected to the double discharge cycle (II + I) show a slightly higher relative density and microhardness than any others. It might be caused by the breakdown of the oxide layers of the powder particles taking place during the configuration II stage, making easier the later electrical current passing when configuration I is applied.
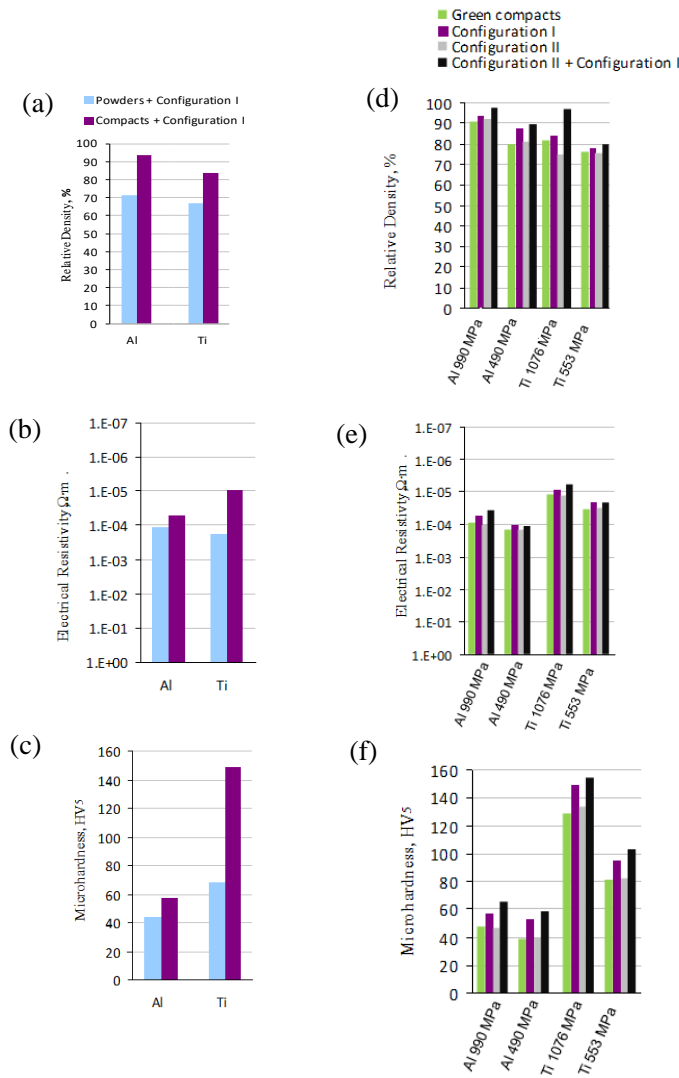


Figure 4. Comparison of (a) relative density, (b) Vickers microhardness and (c) electrical resistivity of high-pressure pre-pressed compacts and compacts consolidated from loose powders by EDC, both with configuration I; and (d) relative density, (e) Vickers microhardness and (f) electrical resistivity of pre-pressed compacts with the two different pressures, consolidated with both configurations (II + I).

Finally, the electrical resistivity of the compacts consolidated with configuration I results very similar to the one obtained after consolidating with configuration II + I, whereas that of the compacts consolidated with the configuration

II is almost the same that the one of the green compacts (Figure 4f). Therefore, the EDC with configuration II does not have an important effect on powders consolidation; however, it may favor the electrical current passing in a subsequent discharge.

### 3.2. Microstructural Study

For the Al compacts, optical micrographs were carried out on a diametrical section of the compact, differentiating two zones: outer (periphery) and centre (Figure 5).

Since the electric current takes preferential paths in its passage through the powder column, a little homogeneous porosity distribution is to be expected. However, the higher porosity observed at the periphery of the diametrical section is increased by the loss of material during the mechanical cutting and metallographic preparation process. This difference is more pronounced in the samples obtained from loose powder, where consolidation is poorer. However, in the samples that were previously pressed, the differences are smaller, due to the greater consistency of these compacts.
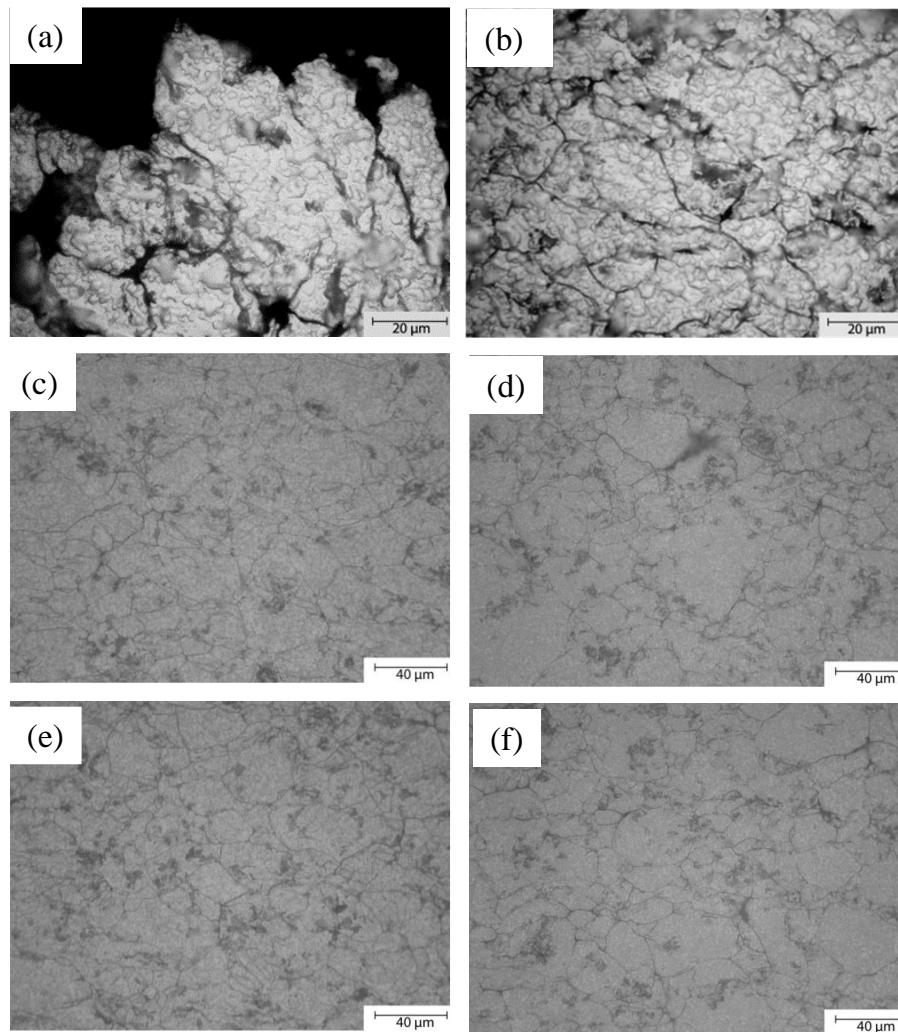


Figure 5. Optical micrographs of the Al compacts: (a) and (b) periphery and centre, respectively, of the compact consolidated from loose powders and discharging with configuration I; (c) and (d) periphery and centre, respectively, of the compact consolidated from a pre-pressed green compact (990 MPa) and subsequent discharge with configuration II; (e) and (f) periphery and centre, respectively, of the compact consolidated from a pre-pressed green compact (990 MPa) and subsequent discharge with configuration II + I.

On the other hand, Figure 7 shows different micrographs taken on fracture surfaces of the different compacts obtained at different pressures: (a) none (loose powder), (b) 490 MPa and (c) 990 MPa. Configuration I was used to

perform the EDC of the compact obtained from loose powder, and a combined configuration (II + I) for the cold-pressed compacts.
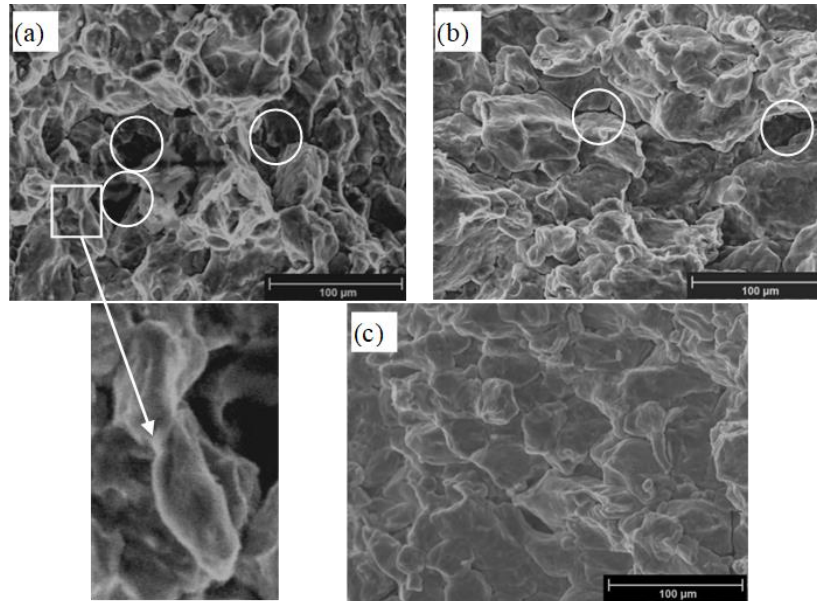


Figure 7. SEM micrographs of Al AS61 compacts: (a) loose powders and configuration I, (b) green compact pressed at 490 MPa and subsequent discharge with configuration (II + I) and (c) green compact pressed at 990 MPa and subsequent discharge with configuration (II + I) and details of the possible joints (micro-welds) between particles.

Figure 7a shows the SEM micrographs of the fracture surface of the compact obtained from loose powder and discharge of the I equipment. It can be seen that, as is typical of compacts obtained from loose powders, the effect of the preferential electric current paths is more clearly manifested, with more porous areas (circled in figure 7a). Inter-particle bonds can be seen, for example, in the squares shown in Figure 7a, although in general, there are not many such bonds across the surface studied.

It can be seen that the compacts pressed at 990 MPa show slightly better consolidation (no significant pore size in Figure 5.11c) than the compacts pressed at 490 MPa (pores circled in Figure 7b) and the compacts that were not previously pressed (clearly higher porosity, circled in Figure 7a). This corroborates the results obtained for the previously measured properties (relative density, electrical resistivity and Vickers microhardness) where it was stated that the compacts pressed at 990 MPa had the lowest relative density and the lowest electrical resistivity, which favoured consolidation. On the other hand, the previously pressed compacts have deformed particles so that no possible joints between them can be seen. However, the compacts that have not been previously pressed do allow some joints between particles to be seen (joints between particles surrounded by a square in Figure 7a, corresponding to the compact obtained from loose powder). In addition, the different morphology of the fracture is clearly seen, being more homogeneous and less porous at higher applied pressure. This is due, as mentioned above, to the fact that the compacts pressed at higher pressure increase the paths for the passage of the current, which improves their consolidation.

As with Al and Ti compacts clearly shows that the central zone of the compact has fewer pores than the periphery. Figure 8 shows, as expected, that the compacts obtained from loose powders and discharging with configuration I present higher porosity than the compacts that were previously pressed.
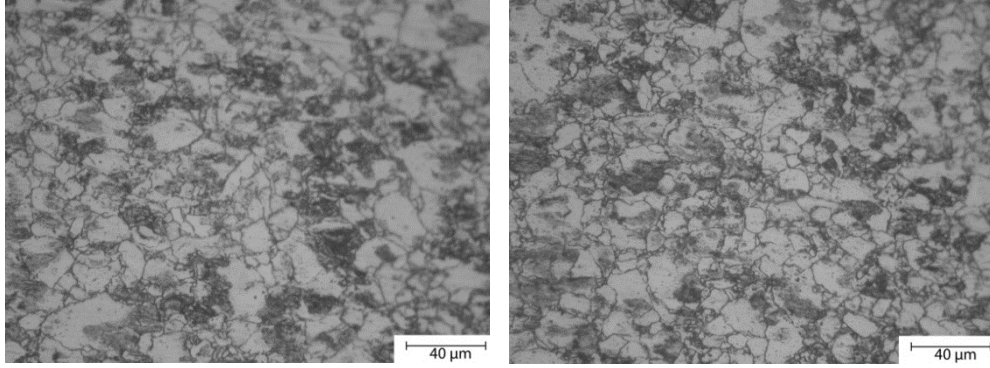
Figure 8: (a) centre and (b) periphery of Ti compact previously pressed at (553 MPa) and with a discharge of combined configuration (II+I) .

Figure 9 shows the micrographs of Ti compacts pre-pressed at 1073 and 553 MPa and subsequent discharge with combined configuration (II + I), and compact obtained starting from loose powders and configuration I discharge. It can be seen that, as before, the most porous compacts are the non-prepressed compacts (circled in Figure 9a), while the pressed compacts show lower porosity. The homogeneity of the pressed compacts is evident in Figure 9b and Figure 9c. The differences in the compacts subjected to different pressures and the same discharge cycle (configuration II + I) are not noticeable in these micrographs. No joints between particles caused by the passage of the electric current can be seen in any of the cases, but it can be observed that the particles of the pressed compacts are deformed due to the pressure to which they have been subjected.
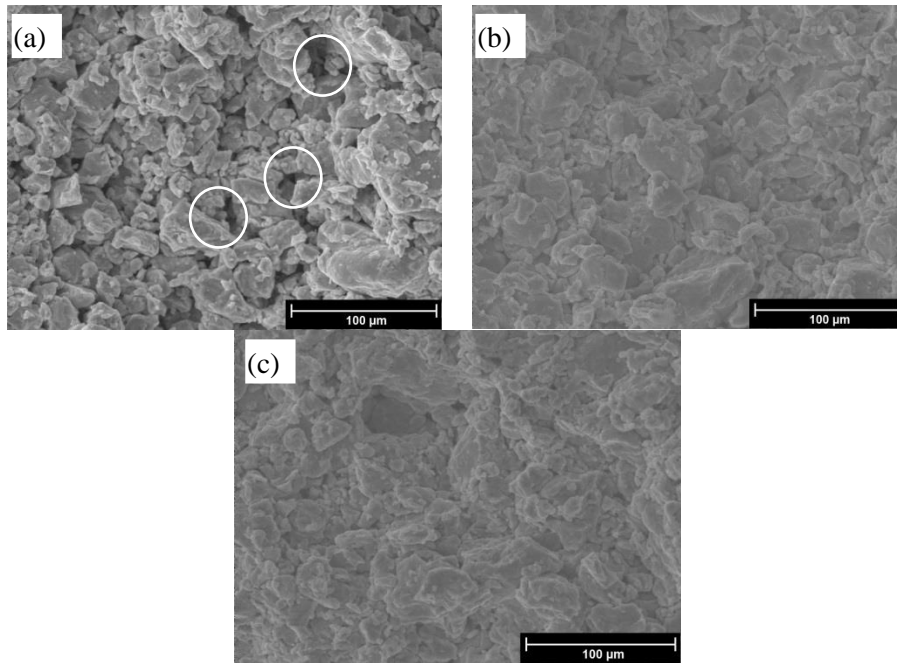


Figure 9 SEM micrographs of Ti compacts: (a) unpressed powders and discharge with configuration I, (b) pre-pressed at 553 MPa compacts and subsequent discharge with a combined modality (II + I) and (c) pre-pressed at 1076 MPa compacts and subsequent combined discharge (II + I).

## 4. Conclusions

Commercial powders of Al and Ti have been consolidated by passing through them an electrical current from a capacitors bank, achieving a low relative density (high porosity).

Pre-compacted powders reach after the EDC process a higher relative density (lower porosity) and higher hardness

than the obtained in compacts prepared starting from loose powder.

The different discharge configurations applied show that configuration II (800 V - 1.1 mF) favors the breaking of the oxide layer covering powder particles, however it has no significant effect on the microhardness and electrical resistivity. On the other hand, configuration I (200 V – 66 mF) has a critical contribution on these properties. The higher microhardness is obtained applying a discharge with a combined configuration (II+I) .

## Acknowledgements

## References

[1] G.F. Taylor. Apparatus for Making Hard Metal Compositions (US Patent no. 1:854-896, 1933).

[2] G.D. Cremer. Powder Metallurgy (US Patent no. 2:355-954, 1944).

[3] W.F. Ross. Method and Apparatus for Making Solid Objects from Metal Powders (US Patent no. 2:372-605, 1945).

[4] F.V. Lenel. Resistance sintering under pressure. *Journal of Metals* 1955; 7 (1):158-167.

[5] K. Okazaki. Electro-discharge consolidation of particulate materials. *Reviews in Particulate Materials* 1994; 2:215-269.

[6] K. Okazaki and M. I. Lifland. Properties of titanium dental implants produced by electro-discharge compaction. *Clinical Materials* 1994; 17 (4):203-209.

[7] J.M. Montes. Modelado de la sinterización por resistencia eléctrica bajo presión de polvos metálicos. (Ph.D. thesis, University of Sevilla, Spain, 2003).

[8] J.M. Montes, J.A. Rodríguez, and E.J. Herrera. Thermal and electrical conductivities of sintered powder compacts. *Powder Metallurgy* 2003; 46 (3):251-256. DOI:10.1179/003258903225008544

[9] J.M. Montes et al. Electrical resistance sintering of M.A. Al-5AlN powders. *Materials Science Forum* 2006; 514-516:1225-1229. DOI: 10.4028/www.scientific.net/msf.514-516.1225

[10] J.M. Montes, F.G. Cuevas, and J. Cintas. Electrical resistivity of metal powder aggregates. *Metallurgical and Materials Transactions B: Process Metallurgy and Materials Processing Science* 2007; 38 (6):957-964. DOI: 10.10I:07/s11663-007-9097-3

[11] M.V. Zamula et al. Electric-Discharge Sintering of TiN-AlN Nanocomposites. *Powder Metallurgy and Metal Ceramics* 2007; 46 (7-8):19-27. DOI: 10.1007/s11106-007-0052-2